MPMI Vol. 19, No. 3, 2006, pp. 330–341. DOI: 10.1094/MPMI-19-0330.

e-Xtra*

Insights into Symbiotic Nitrogen Fixation in *Medicago truncatula*

Mesfin Tesfaye,[1] Deborah A. Samac,[1,2] and Carroll P. Vance[2,3]

[1]Department of Plant Pathology, University of Minnesota, St. Paul 55108, U.S.A.; [2]United States Department of Agriculture–Agricultural Research Service Plant Science Research Unit, St. Paul, MN 55108, U.S.A.; [3]Department of Agronomy and Plant Genetics, University of Minnesota, St. Paul 55108, U.S.A.

Submitted 3 August 2005. Accepted 3 November 2005.

In silico analysis of the *Medicago truncatula* gene index release 8.0 at The Institute for Genomic Research identified approximately 530 tentative consensus sequences (TC) clustered from 2,700 expressed sequence tags (EST) derived solely from *Sinorhizobium meliloti*-inoculated root and nodule tissues. A great majority (76%) of these TC were derived exclusively from nitrogen-fixing and senescent nodules. A cDNA filter array was constructed using approximately 58% of the in silico-identified TC as well as cDNAs representing selected carbon and nitrogen metabolic pathways. The purpose of the array was to analyze transcript abundance in *M. truncatula* roots and nodules following inoculation by a wild-type *S. meliloti* strain, a mutant strain that forms ineffective nodules, an uninoculated root control, and roots following nitrate or ammonium treatments. In all, 81 cDNAs were upregulated in both effective and ineffective nodules, and 78% of these cDNAs represent in silico-identified TC. One group of in silico-identified TC encodes genes with similarity to putative plant disease resistance (*R*) genes of the nucleotide binding site–leucine-rich repeat type. Expression of *R* genes was enhanced in effective nodules, and transcripts also were detected in ineffective nodules at 14 days postinoculation (dpi). Homologous *R* gene sequences also have been identified in the *Medicago* genome. However, their functional importance in nodules remains to be established. Genes for enzymes involved in organic acid synthesis along with genes involved in nitrogen metabolism were shown to be coexpressed in nitrate-fed roots and effective nodules of *M. truncatula*.

Nitrogen (N) is the mineral nutrient needed in greatest abundance by plants, and most plant species can utilize a wide range of N species, including applied nitrate and ammonium fertilizers (Crawford 1995). DNA arrays have been used to identify *Arabidopsis* and tomato genes that respond to nitrate nutrition (Scheible et al. 2004; Wang et al. 2001, 2003). Addition of nitrate to *Arabidopsis,* tomato, and tobacco induces genes involved in organic acid metabolism and nitrate uptake, reduction, and transport (Scheible et al. 1997, 2004; Wang et al. 2001, 2003). An important aspect of legumes, including *Medicago truncatula,* is their unique ability to obtain N via bacterial symbiosis with soil bacteria, collectively called rhizobia. This extremely host-specific bacterial symbiosis results in the formation of a completely novel plant organ, the root nodule, following the perception of secreted rhizobial Nod factors. The root nodule houses the nitrogen-fixing rhizobia and allows the host plant to acquire biologically fixed nitrogen. The acquisition of nitrogen in symbiosis with soil bacteria triggers a wide variety of molecular and physiological changes in the host plant. Because of the close relationship of *M. truncatula* with the cultivated tetraploid alfalfa (*M. sativa*) and its relatively small genome size, *M. truncatula* is being used as a model plant for studies of legume biology and has been the subject of structural and functional genomics work (Cook 1999). The international effort in plant genomics has positioned *M. truncatula* as a resource plant for understanding agronomic traits of importance to forage and grain legumes (Thoquet et al. 2002).

The *M. truncatula* expressed sequence tag (EST) database at The Institute for Genomic Research (TIGR) contains some 227,000 EST sequences derived from over 55 cDNA libraries of different plant tissues exposed to several treatments and conditions. At TIGR, individual overlapping EST have been clustered into tentative consensus sequences (TC) that represent putative genes. Using in silico (electronic Northern) analysis of the *M. truncatula* Gene Index (MtGI) release 4.0 in September 2001, Fedorova and associates (2002) identified approximately 340 TC belonging to several functionally important categories that, putatively, were expressed solely in root nodules. Two groups of unusual nodule-specific TC were identified: calmodulin-like (CaM-like) proteins and cysteine-cluster containing proteins (CCPs) (Fedorova et al. 2002). A selected number of nodule-specific CCPs were shown experimentally to be expressed solely in developing and mature nodules (Mergaert et al. 2003), and computational analysis by Graham and associates (2004) suggests that *Medicago* CCPs may be found only in legumes. Nevertheless, since the previous reporting of the nodule-specific transcripts, the MtGI was supplemented with approximately 82,000 more *M. truncatula* EST, increasing the total number of TC by 3,919 to the current total of 18,612 TC (MtGI release version 8.0, January 2005). In a preliminary in silico analysis of the MtGI release 7 in May 2003 to evaluate consequences of deeper sequencing, we noted that i) the number of EST clustered in some of the nodule-specific TC was increased with additional EST derived exclusively from symbiotic root and nodule tissues; ii) although some TC remained as

Corresponding author: Mesfin Tesfaye; 495 Borlaug Hall, 1991 Upper Buford Circle; E-mail: Mesfin.Tesfaye-1@umn.edu; Telephone: +1-612-625-1728; Fax: +1-651-649-5058;

*The *e*-Xtra logo stands for "electronic extra" and indicates the HTML abstract available on-line contains supplemental material not included in the print edition.

This article is in the public domain and not copyrightable. It may be freely reprinted with customary crediting of the source. The American Phytopathological Society, 2006.

nodule specific, they were re-annotated for putative gene function; and iii) the number of EST clustered in some nodule-specific TC was increased with additional EST from non-nodule tissue cDNA libraries. These observations provided the impetus to undertake an in silico analysis using the most recent MtGI database and identify and update the list of bacterial symbiosis-specific *M. truncatula* TC. We also have studied the abundance of selected transcripts elicited during symbiotic nitrogen fixation using a cDNA filter array containing in silico-identified cDNAs as well as cDNAs representing selected genes for enzymes involved in carbon (C) and nitrogen metabolic pathways. Transcript abundance of genes in *M. truncatula* root nodules following inoculation with a wild-type effective *Sinorhizobium meliloti* strain (Nod^+Fix^+) and a mutant *S. meliloti* strain that forms ineffective nodules (Nod^+Fix^-) was examined. We also investigated whether or not nitrate and ammonium fertilizer additions lead to changes in gene transcription in *M. truncatula* roots. The present study represents the first report of cDNA array analysis performed with *M. truncatula* to identify plant genes expressed in response to different nitrogen sources. We show that a customized array using available cDNAs from the model legume *M. truncatula* such as reported here gives further insights into N and carbon metabolism in legumes in general and *M. truncatula* in particular.

RESULTS AND DISCUSSION

In silico analysis of *Sinorhizobium*-inoculated tissue-specific transcripts.

Among the 55 EST libraries represented in release 8.0 of MtGI, 9 libraries comprising 32,972 EST (14.5% of the *M. truncatula* EST database) were prepared from mRNA extracted from *S. meliloti*-inoculated roots and N-fixing and senescent nodules of *M. truncatula*. These cDNA libraries can be categorized into three major nodule-developmental stages: the inoculated root at 1 to 3 days postinoculation (dpi) (T1841, T1510, and T1707), young and N-fixing nodules at 4 to 30 dpi (5519, #G8L, 2764, 4047, and T1617), and senescent nodules at 40 and 60 dpi (T10109). One important development of *M. truncatula* genomics has been the ability to identify nodule-specific transcripts by electronic analysis (Fedorova et al. 2002; Graham et al. 2004; Journet et al. 2002; Mergaert et al. 2003). Due to considerable additions of *Medicago* EST by the *Medicago* community and the updating of the MtGI by TIGR, the in silico search in the present study was conducted with the aim of updating the list of those TC that were clustered with EST derived exclusively from inoculated-root or nitrogen-fixing and senescent nodules. We identified 533 TC clustered from 2,649 EST solely from *S. meliloti*-inoculated root- and nodule-cDNA libraries of *M. truncatula* (Table 1). With regard to stages of nodule development, 10% of these TC appear to be induced during the early stages of nodule development (1 to 3 dpi), whereas the expression of 76% of the TC was exclusively in N-fixing and senescent nodules (4 to 40 dpi) (Table 1). Transcription of the remaining 13% of the in silico-identified TC was initiated early in the nodulation process and continued to late nodulation stages (Table 1).

Although 48% (253 TC) of the in silico-identified TC showed similarity to previously deposited sequences in GenBank, approximately 52% of the TC appear to be novel or showed similarity to genes of unknown function (Table 1). In silico-identified TC that showed high similarity to previously characterized genes belong to several functional categories, including host resistance and defense response genes (5.1%), nodulins and hemoglobins (8.6%), transporters (3.4%), and signal transduction (6.2%), among others.

Expression patterns of in silico-identified TC using cDNA array and RNA blots showed that transcript abundance of TC composed of five or more EST per TC verified enhanced expression in nodules (Fedorova et al. 2002) and, thereby, indicated abundant transcription in nodules. It appears that only 22% (118 TC) of the inoculated root and nodule TC consist of five or more EST per TC (Table 1). Therefore, it is necessary to carry out experimental validation of in silico-identified TC to confirm transcript abundance and patterns of transcription during nodule development.

To study transcriptional events elicited during symbiotic nitrogen fixation as well as nitrate and ammonium nutrition, we spotted 576 cDNAs representing 493 TC in a filter array. Of these, 296 cDNAs representing 287 TC (58.2% of the in silico-identified TC) were identified by our in silico analysis as being clustered from EST obtained exclusively from *Sinorhizobium*-inoculated tissue cDNA libraries. These and additional cDNAs were chosen to represent genes for signal transduction; host stress and defense response; organic acid metabolism; transport function; nitrogen, carbon, and other primary metabolic pathways; and secondary metabolism, as well as genes with unknown function or no annotation.

Transcript abundance of *Medicago* roots and nodules following treatments with different nutrient nitrogen sources.

For inoculation treatments, *M. truncatula* plants were inoculated with wild-type *S. meliloti* strain 102F51 and a mutant *S. meliloti* strain T202. The wild-type *S. meliloti* strain 102F51

Table 1. Distribution of in silico-identified *Sinorhizobium*-inoculated tissue-specific transcripts by nodule development and functional category (*Medicago truncatula* Gene Index release 8.0, January 2005)[a]

Category	Number of TC (EST) in				Total TC (%)	With ≥5 EST[b]
	Inoc. roots	Nodules	Inoc. roots and nodules	Total		
Host resistance and defense response	9 (25)	17 (47)	1 (2)	27 (74)	5.1	3
Known nodulins and hemoglobins	2 (10)	29 (458)	15 (275)	46 (743)	8.6	30
Transport function	3 (7)	12 (47)	3 (8)	18 (62)	3.4	2
Signal transduction	5 (13)	20 (92)	8 (36)	33 (141)	6.2	8
Metabolism	8 (19)	14 (49)	4 (27)	26 (95)	4.9	5
Cell structure and maintenance	5 (10)	6 (16)	1 (3)	12 (29)	2.3	1
Protein synthesis and processing	4 (9)	8 (21)	0 (0)	12 (30)	2.3	1
Gene expression and RNA processing	2 (4)	5 (10)	1 (6)	8 (20)	1.5	2
Growth and hormone related function	1 (2)	2 (5)	1 (3)	4 (9)	0.8	0
Miscellaneous function	2 (5)	56 (275)	9 (43)	67 (323)	12.6	15
Unknown function or no homology	14 (36)	238 (992)	28 (94)	280 (1,122)	52.5	51
Total	55 (140)	407 (2,012)	71 (497)	533 (2,649)	…	118
Total TC (%)	10.3	76.4	13.3	100.0	…	22.1

[a] TC = tentative consensus sequences, EST = expressed sequence tags, Inoc. = inoculated.
[b] Number of TC with five or more EST.

induces nitrogen-fixing nodules that are relatively large in size and relatively few in number (Nod^+Fix^+) on both *M. truncatula* and *M. sativa*. The mutant *S. meliloti* strain T202 is defective in microaerobic *nif*A induction and produces relatively much smaller and numerous whitish-green nodules that do not fix nitrogen (Nod^+Fix^-) (Virts et al. 1988). Both effective and bacterial-conditioned ineffective nodules contain *S. meliloti* cells in nodule tissues, but those elicited by T202 contain degenerating bacteriodes (Virts et al. 1988). Gene expression patterns were evaluated between nodules of *S. meliloti*-inoculated plants at 14 dpi and roots of uninoculated control plants that grew in parallel. In *M. truncatula*, visible emergence of root nodules resulting from inoculation with wild-type effective *Sinorhizobium* occurs between 6 and 9 dpi (S. Miller and C. Vance, *unpublished*). This period coincides with the onset of nitrogenase activity, estimated by the reduction of acetylene to ethylene in a gas chromatography analysis (S. Miller and C. Vance, *unpublished*). By using an effective wild-type strain and an ineffective mutant strain as inoculants and harvesting nodules at 14 dpi (well after fixation of atmospheric nitrogen to ammo-

Table 2. Significantly expressed cDNAs for signaling, plant disease resistance, host disease response, and secondary metabolism in effective and ineffective nodules and nitrate and ammonium treated roots of *Medicago truncatula*[a]

				N/R[b]		R/R[c]	
TC no.[d]	EST no.	Annotation	*P* value	Fix^+	Fix^-	Nitrate	Ammonium
*TC99871	EST393509	bZIP transcription factor ATB2	0.0012	3.5	1.2	1.0	0.7
TC106874	EST316359	Calmodulin	0.0185	1.1	0.7	1.4	0.7
*TC107257	EST483431	Calmodulin-like protein 1	0.00001	4.3	2.7	0.8	0.7
*TC107926	EST391888	Calmodulin-like protein 2	0.0004	2.7	1.8	1.2	0.7
*TC101807	EST429680	Calmodulin-like protein 3	0.0398	4.0	2.3	0.8	0.8
*TC102961	EST482246	Calmodulin-like protein 5	0.0438	1.1	1.0	1.2	0.5
*TC102961	EST485196	Calmodulin-like protein 5	0.00002	4.8	2.2	1.2	1.0
*TC95911	EST484542	Calmodulin-like protein 6b	0.0001	3.2	1.5	1.3	1.0
TC106641	EST457853	Cold and drought-regulated protein CORA	0.0373	1.7	1.1	1.2	0.7
TC106356	EST431072	dnaK-type molecular chaperone PHSP1	0.0123	2.3	1.0	1.2	0.9
TC106356	EST430358	dnaK-type molecular chaperone PHSP1	0.0326	2.4	0.9	1.3	0.9
TC107124	EST458151	EF-hand calcium binding protein like	0.0248	1.6	1.5	1.1	0.7
*TC111690	EST482833	G protein-coupled receptor GPR1	0.0001	4.1	2.1	1.0	0.8
TC105444	EST590759	Glutamate receptor	0.0073	2.0	1.1	0.9	0.5
TC108036	EST484439	GSK-3 like protein MsK4	0.0006	3.3	1.8	0.9	0.7
TC109213	EST484488	Kunitz proteinase inhibitor-1	0.0002	3.5	1.7	1.2	0.7
TC103085	EST590099	SET domain protein SDG117	0.0267	1.9	1.5	0.8	0.6
TC99020	EST431756	Protein phosphatase 2C	0.0361	1.6	1.2	1.1	0.7
*TC112320	EST483859	Protein phosphatase 2C β isoform	0.00005	4.4	2.3	1.0	0.5
*TC96630	EST482341	Remorin-like protein	0.005	4.9	2.2	0.9	0.7
*TC103882	EST332771	S glycoprotein	0.0087	2.1	1.1	1.2	0.6
*TC106116	EST430688	STE11 protein kinase homolog NPK1	0.0148	2.4	1.7	1.3	0.6
TC95842	EST314673	SVP-like floral repressor	0.0178	3.7	1.7	1.5	0.8
*TC95981	EST392070	Transcription factor	0.0001	4.7	2.3	1.2	0.6
TC94534	EST482381	Transcription factor Myb1	0.0195	1.3	0.9	1.6	0.7
TC94535	EST429833	Transcription factor Myb1	0.0077	1.7	0.8	2.0	0.8
TC94210	EST458474	Cationic peroxidase	0.0151	1.7	1.4	1.2	0.5
TC107261	EST397202	Peroxidase precursor	0.0214	2.0	1.4	1.1	0.7
TC108234	EST485645	Peroxidase precursor	0.00002	4.6	2.3	0.9	0.5
*TC111329	EST432510	Probable glutathione peroxidase	0.0206	1.5	0.9	1.2	0.4
*TC108455	EST483279	Chitin biosynthesis protein CHS5.	0.00004	4.9	2.9	1.1	0.5
TC101625	EST430516	Cysteine protease 5	0.0215	1.2	0.8	1.3	0.5
*TC100440	EST430316	Cysteine protease 8	0.0044	1.9	1.4	1.0	0.4
*TC100443	EST431401	Cysteine protease 8	0.0009	1.5	2.6	1.2	1.1
*TC98138	EST430401	Cysteine protease 8	0.0084	1.7	1.2	1.3	0.4
TC100972	EST483929	Cysteine proteinase	0.0001	4.1	2.8	0.8	0.9
TC93993	EST456551	Cysteine proteinase 15A precursor	0.0281	0.9	0.7	1.2	0.6
*TC101983	EST484919	Cysteine proteinase inhibitor	0.0005	2.9	1.7	1.1	0.8
TC106659	EST457404	Dehydrin-cognate	0.0209	1.9	1.0	1.2	0.5
TC106660	EST485274	Dehydrin-cognate	0.0497	1.5	0.8	1.4	0.6
TC107039	EST484821	Superoxide dismutase (Mn) precursor	0.0054	2.6	1.3	1.5	0.9
*TC102542	EST316627	O-antigen polymerase Wzy	0.00001	4.2	2.8	0.8	0.8
TC100966	EST334746	Environmental stress-induced protein	0.0023	3.1	1.4	1.3	0.6
TC94441	EST315404	Glutaredoxin	0.0013	3.0	1.7	1.4	0.9
*TC105815	EST332500	Disease resistance protein like	0.0012	2.8	1.8	1.2	0.8
TC97948	EST506462	Disease resistance-like protein	0.0409	2.0	1.2	1.2	0.8
TC98670	EST398028	Putative resistance protein	0.0005	4.8	2.1	1.0	0.8
*TC104261	EST334019	Putative TIR-NBS type R protein	0.0377	1.5	1.0	0.9	0.6
TC98532	EST397499	Resistance protein LM12	0.0084	2.3	1.6	1.1	0.5
TC102579	EST432436	Chalcone synthase 1B	0.0019	2.8	1.3	1.0	0.5
TC95934	EST314580	Isoflavone 7-O-methyltransferase 9 (IOMT-9)	0.0042	2.8	1.4	1.0	0.7
TC106939	EST304972	Isoflavone synthase	0.0475	3.2	2.0	1.4	0.5
TC102835	EST432395	Flavanone 3-hydroxylase	0.0106	3.1	1.9	0.9	0.5

[a] Tentative consensus sequence (TC) and expressed sequence tag (EST) numbers correspond to The Institute for Genomic Research *M. truncatula* Gene Index version 8.
[b] N/R denotes mean nodule/uninoculated root expression ratio for effective nodules (Fix^+) and ineffective nodules (Fix^-).
[c] R/R denotes mean expression ratios of nitrate- or ammonium-treated root/KCl-treated roots.
[d] Asterisk (*) indicates identified as *Sinorhizobium* inoculated tissue-specific by in silico analysis.

nium by effectively nodulated plants is assured), we expected to show transcriptional profiles during symbiotic nitrogen fixation. The experiment also included treatments that evaluated transcript abundance of *M. truncatula* roots after nitrate or ammonium was added for 24 h to plants that were N starved for 20 days. Reference plants received KCl for 24 h.

Analysis of variance (ANOVA) done on gene expression ratios derived from three replicates showed that transcript abundance of 281 EST was significantly different ($P < 0.05$) among effective nodules, ineffective nodules, and nitrate- and ammonium-fed roots (Tables 2 to 4). In this report, we use the term "upregulated expression" to refer to an expression ratio of 2- or more fold; otherwise, "enhanced expression" is used to refer to those probes with a 1.5- to 1.9-fold expression ratio. Downregulated genes are those with 0.5- or less fold change in gene expression. It was found that 81 cDNAs showed upregulated expression in both effective and bacterial-controlled ineffective nodules (Tables 2 to 4). cDNAs that were upregulated in both nodule tissues include genes for signaling, host defense response and secondary metabolism, known nodulins, transport function, primary metabolism, and cDNAs with biological function unknown, including 24 cDNAs that belong to the CCPs. In addition, 54 cDNAs of the spotted CCPs on the macroarry showed strong expression in Nod^+Fix^+ nodules.

Compared with the increased number of transcripts induced in nodules, there were only 37 cDNAs that showed upregulated or enhanced expression in nitrate-fed roots (Tables 2 to 4). Of these, 12 cDNAs showed greater transcript abundance in nitrate-fed roots compared with effective nodules. In contrast, addition of ammonium to N-starved *M. truncatula* plants re-

Table 3. Significantly expressed cDNAs encoding known nodulins and transport function proteins in effective and ineffective nodules as well as in nitrate- and ammonium-fed roots of *Medicago truncatula*[a]

				N/R[b]		R/R[c]	
TC no.[d]	EST no.	Annotation	*P* value	Fix^+	Fix^-	Nitrate	Ammonium
*TC106591	EST431616	Leghemoglobin	0.0013	2.8	1.6	0.8	0.5
*TC106578	EST483115	Leghemoglobin 2	0.0007	2.9	1.4	0.7	0.3
*TC106578	EST484248	Leghemoglobin 2	0.0007	2.8	1.3	0.9	0.4
*TC106587	EST391855	Leghemoglobin	0.0019	2.3	1.3	0.8	0.7
TC106592	EST481770	Leghemoglobin 1	0.0007	3.3	1.4	0.6	0.3
TC106593	EST484054	Leghemoglobin	0.0009	2.6	1.5	0.9	0.5
*TC100587	EST484324	Leghemoglobin 29	0.0190	2.0	1.3	1.1	0.9
*TC100586	EST484684	Leghemoglobin 29	0.0009	3.0	2.0	0.9	0.6
*TC100432	EST484492	Early nodule-specific protein	0.000003	6.9	3.9	1.2	0.9
*TC101825	MTNAK80TKM	ENOD12	0.00004	4.4	2.5	0.8	0.6
*TC107339	EST391681	ENOD18	0.0095	2.2	1.2	1.2	1.0
*TC107339	EST484743	ENOD18	0.000004	4.9	2.2	1.6	0.7
*TC100731	EST431276	ENOD20	0.0374	2.5	1.5	1.7	0.7
*TC100731	EST485371	ENOD20	0.0140	2.3	1.8	1.0	0.7
TC100789	EST391799	MtN1	0.0010	3.7	1.9	1.7	1.1
*TC102820	EST393442	MtN17	0.0001	3.1	1.4	0.5	0.2
*TC100596	EST484646	MtN22	0.0021	2.3	1.5	1.1	0.4
*TC107014	EST483909	MtN22	0.0003	2.8	1.9	1.0	0.5
*TC95958	EST484918	MtN26	0.0038	2.7	1.5	1.1	0.7
*TC108339	EST485161	MtN28	0.0453	1.4	1.0	1.0	0.6
*TC107188	EST484058	MtN29	0.0011	2.7	1.7	1.1	0.7
*TC102839	EST431611	Nms22	0.0002	3.6	2.0	1.9	0.7
TC101065	EST429437	Nodule-specific glycine-rich protein 2A	0.0026	2.8	2.1	1.0	0.6
*TC107718	EST483631	Nodule-specific glycine-rich protein 3	0.0007	4.1	2.5	1.1	0.8
*TC101177	EST482622	Nodulin 14 precursor	0.000002	5.2	3.0	0.9	0.8
*TC103322	EST431043	Nodulin 14 precursor	0.0140	1.1	0.5	1.1	0.4
*TC103042	EST485266	Nodulin 14 precursor	0.0237	2.6	1.9	1.3	1.2
*TC106696	EST393910	Nodulin 25	0.0012	2.2	1.6	1.0	0.6
*TC106696	EST393913	Nodulin 25	0.0002	2.9	1.3	0.9	0.5
*TC109561	EST485034	Nodulin 25	0.00004	4.2	1.8	0.8	0.3
*TC103632	EST429323	2-on-2 hemoglobin	0.0264	1.7	1.5	1.1	0.8
TC110826	EST394058	ABC transporter ATP-binding component	0.0019	2.2	1.6	1.0	0.4
*TC107616	EST430001	ABC transporter ATP-binding component	0.0411	1.4	0.9	1.0	0.5
*TC111233	EST482317	Amino acid transport protein AAT1	0.0056	3.3	1.0	1.4	1.1
TC106619	EST306131	Aquaporin	0.0131	2.9	1.7	1.0	1.1
TC100289	EST315081	Aquaporin protein PIP1	0.0066	2.7	1.7	0.7	0.5
TC102991	EST393541	Calcium-binding transporter-like protein	0.0366	2.6	1.9	0.9	0.7
TC102991	EST393468	Calcium-binding transporter-like protein	0.0048	2.2	1.2	1.1	0.8
*TC100607	EST430869	Enterochelin ABC transporter permease	0.0016	2.3	1.6	1.1	0.7
*TC101768	EST482728	Hexose transporter	0.0228	2.4	1.7	1.4	0.8
TC107287	EST482950	Hexose transporter	0.0001	4.2	2.8	1.5	1.1
*TC107904	EST482014	Hexose transporter	0.0000	4.4	1.6	1.2	0.7
*TC112178	EST333640	High affinity sulfate transporter 2	0.0311	2.1	1.1	1.2	0.7
TC108692	EST392314	Nitrate transporter	0.0030	4.0	2.4	1.1	0.9
TC100832	EST457462	Sodium-dependent transporter-like	0.0271	3.2	2.3	1.3	0.7
*TC104863	EST482209	Sulfate transporter protein-like	0.0001	3.1	1.2	1.3	0.4
TC101252	EST483708	Sulfate transporter-like protein	0.0009	4.4	2.1	0.9	0.7t

[a] Tentative consensus sequence (TC) and expressed sequence tag (EST) numbers correspond to The Institute for Genomic Research *M. truncatula* Gene Index version 8.
[b] N/R denotes mean nodule/uninoculated root expression ratio for effective nodules (Fix^+) and ineffective nodules (Fix^-).
[c] R/R denotes mean expression ratios of nitrate- or ammonium-treated root/KCl treated roots.
[d] Asterisk (*) indicates identified as *Sinorhizobium* inoculated tissue-specific by in silico analysis.

sulted in no change in expression or weakly to strongly downregulated expression of cDNAs (Tables 2 to 4).

Expression of known nodulins in *Medicago* nodules and validation of macroarray expression data.

In the MtGI release 8.0 EST database, 46 nodulin and hemoglobin TC clustered from 735 EST appear to be expressed specifically during bacterial symbiosis. Of these, 30 nodulin and hemoglobin TC were clustered from five or more EST per TC, indicating that these transcripts are highly expressed in nodules. In conformity to published reports, a series of previously known nodulins as well as leghemoglobin cDNAs that are known to be restricted to nitrogen fixation (Appleby 1984; Ott et al. 2005) displayed enhanced expression in effective nodules (Table 3). Of the 10 leghemoglobin cDNAs spotted on the array, eight cDNAs showed upregulated expression in Nod^+Fix^+ nodules (Table 3). Additionally, 15 nodulin cDNAs showed upregulated expression in Nod^+Fix^+ nodules, including nodulin 25 (TC106696 and TC109561) and MtN22 (TC100596 and TC107014), among others (Table 3).

We also employed quantitative reverse-transcription polymerase chain reaction (qRT-PCR) to verify the macroarray results. In 10 of the 13 samples for which validation was performed, the qRT-PCR analysis supported the trends observed in the expression pattern from the macroarray analysis (Table 5). However, the expression ratios determined by qRT-PCR analysis were higher than the expression ratios determined by the macroarray analysis, in some instances with 10-fold differences (Table 5). The discrepancies may reflect that the qRT-PCR is a more dynamic technique than transcript profiling using cDNA arrays.

Plant disease resistance, host defense response, and signal transduction genes are induced in *Medicago* nodules.

For root nodule symbiosis, an exchange of signal molecules between the host and rhizobia is required. After root colonization, rhizobia enter roots of *Medicago* via root hairs and migrate to the root cortex via infection threads and induce the formation of nodules typically in the susceptible region of the root. It is generally thought that a compatible symbiotic interaction involves an inhibition of host defense mechanisms to permit the establishment of N-fixing soil bacteria within the host cells (Mithofer 2002). However, the present study and previously published work by others have reported enhanced

Table 4. Significantly expressed genes for primary metabolism, including organic acid synthesis and nitrogen assimilation, in effective and ineffective nodules as well as nitrate- and ammonium-treated roots of *Medicago truncatula*[a]

				N/R[b]		R/R[c]	
TC no.[d]	EST no.	Annotation	*P* value	Fix^+	Fix^-	Nitrate	Ammonium
*TC100173	EST393902	Carbobonic anhydrase	0.0054	2.3	1.3	1.2	0.6
TC100769	EST482182	2-oxoglutarate dehydrogenase E2 subunit	0.0052	2.9	2.1	1.6	0.7
TC100769	EST484912	2-oxoglutarate dehydrogenase E2 subunit	0.005	0.6	0.6	1.6	0.7
TC94299	EST433466	Aminotransferase 2	0.0136	1.8	0.8	0.9	0.7
TC94299	EST459080	Aminotransferase 2	0.0014	2.5	2.6	1.4	0.7
TC100393	EST484092	Asparagine synthetase	0.0058	2.5	1.1	2.4	1.2
TC100391	EST484277	Asparagine synthetase	0.0001	3.1	0.8	3.8	1.3
TC94272	EST433452	Ferredoxin I	0.0001	4.0	2.2	0.9	0.5
TC94780	EST315811	Glutamate synthase (NADH-GOGAT)	0.0005	0.8	0.7	2.2	0.9
TC106913	EST392441	Glutamine synthetase	0.0225	1.7	1.0	5.2	1.5
TC100672	EST392190	Nitrite reductase precursor	0.000002	3.0	1.6	10.9	1.7
TC94246	EST335462	Carbonic anhydrase	0.0001	3.5	2.4	1.4	0.6
TC107007	EST485484	Citrate synthase	0.0204	1.7	1.5	1.4	0.6
TC95758	EST316070	Citrate synthase glyoxysomal precursor	0.0362	1.7	1.2	1.5	0.9
TC94329	EST335885	Isocitrate dehydrogenase [NADP]	0.0303	1.0	0.7	1.1	0.5
TC107189	EST484269	Malate dehydrogenase precursor	0.0026	3.0	1.9	2.0	1.0
TC100429	EST484621	Malate dehydrogenase, cytoplasmic	0.0024	1.2	0.8	1.9	1.1
TC100430	EST484499	Malate dehydrogenase, cytosolic	0.0123	1.4	0.9	1.6	0.8
TC94390	EST458395	Malate dehyrogenase, glyoxysomal	0.0194	2.2	1.3	1.5	0.8
TC94196	EST334814	Phosphoenolpyruvate carboxylase (PEPC)	0.0032	1.7	0.9	1.6	0.6
TC108608	EST485425	Phosphoenolpyruvate carboxylase kinase	0.0013	2.5	1.8	2.9	0.7
TC101044	EST482958	Succinyl-CoA synthase	0.0044	1.0	0.8	1.7	0.9
TC106499	EST431116	Neutral invertase	0.0043	2.2	1.1	1.0	0.8
TC100410	EST392153	Sucrose synthase	0.0004	1.2	1.0	2.4	1.1
TC100410	EST430478	Sucrose synthase	0.0001	1.4	1.0	2.9	1.0
TC94345	EST483187	Fructokinase	0.0301	0.7	0.7	1.5	1.1
TC100600	EST458368	Fructose-bisphosphate aldolase, cytoplasmic	0.0006	3.3	2.0	0.6	0.5
TC106518	EST482370	Glyceraldehyde 3-phosphate dehydrogenase, cytosolic	0.026	1.8	1.1	1.3	0.8
TC100701	EST315973	UDP-D glucuronate 4-epimerase	0.0212	2.3	2.4	1.1	0.7
TC94414	EST392348	NADP-glyceraldehyde-3-phosphate dehydrogenase	0.0277	2.2	1.2	1.1	0.8
*TC96185	EST393366	Cytochrome b	0.00002	5.1	3.3	0.9	0.8
*TC102093	EST482549	Cytochrome b	0.0001	3.4	1.8	0.9	0.6
TC100154	EST433448	Photosystem II type I chlorophyll a/b-binding protein	0.0007	3.0	1.5	1.1	1.1
*TC95126	EST482660	PTS system fructose-specific IIBC component	0.00001	4.2	2.1	1.1	0.8
TC93923	EST433496	Ribulose 1,5-bisphosphate carboxylase	0.0001	3.9	1.9	1.1	0.6
TC106337	EST433578	Hydroxyproline-rich glycoprotein precursor	0.0133	1.6	0.8	1.1	0.3
*TC103235	EST482450	Integral membrane protein	0.0001	3.4	2.1	1.4	0.7
TC107338	EST393474	Actin	0.0352	1.7	1.0	1.2	0.8

(*continued on next page*)

[a] Tentative consensus sequence (TC) and expressed sequence tag (EST) numbers correspond to The Institute for Genomic Research *M. truncatula* Gene Index version 8.
[b] N/R denotes mean nodule/uninoculated root expression ratio for effective nodules (Fix^+) and ineffective nodules (Fix^-).
[c] R/R denotes mean expression ratios of nitrate- or ammonium-treated root/KCl treated roots.
[d] Asterisk (*) indicates identified as *Sinorhizobium* inoculated tissue-specific by in silico analysis.

transcription of host stress and defense response genes in nodules (Colebatch et al. 2004; Gamas et al. 1998; Kouchi et al. 2004; Manthey et al. 2004; Yahyaoui et al. 2004). Twenty-seven TC with similarity to host disease resistance (*R*) and defense response genes were identified by in silico analysis. Of these, eight TC (TC96037, TC96816, TC98891, TC104195, TC104261, TC105815, TC110511, and TC111855) share protein sequences similar to *R* genes with the nucleotide binding site–leucine-rich repeat (NBS-LRR). Six of these TC were clustered from 14 EST derived exclusively from inoculated root cDNA libraries (2 to 4 dpi), whereas two TC were clustered from five EST derived from nodule and inoculated root cDNA libraries. Interestingly, all in silico-identified TC with similarity to *R* genes were clustered with two or three EST, suggesting a relatively low level of expression in nodules.

Taking advantage of the publicly available *Medicago* genome sequences, we took a bioinformatics approach to identify candidate *R* gene sequences. Using deduced amino acid sequences of the in silico-identified TC as queries, the BLASTP algorithm (E value = 0.001) as provided by the chromosome visualization tool (CViT) was used for the search. The BLAST search identified approximately 178 BAC sequence hits, but only 34 candidate gene sequences predicted from 17 *Medicago* BACs were verified by the International *Medicago* Genome Annotation Group consortium (IMGAG). The homologous *Medicago* genome sequences encode the conserved NBS domain of *R* genes (Meyers et al. 1999). The amino acid motifs located on the NBS domain have been used to distinguish the toll and interleukin-1 receptor (TIR) and non-TIR NBS-LRR subfamilies of *R* genes (Meyers et al. 1999; Zhou et al. 2002). The deduced amino acid NBS domain of 40 sequences were aligned using ClustalW: 9 *R* gene sequences from GenBank, 29 sequences from *Medicago* genome, and 2 of the in silico-identified TC from MtGI. Only TC96816 and TC98891 of the in silico-identified TC contained nucleotide sequences spanning the phosphate loop (P-loop) and GLPL motifs of the NBS domain. A parsimony tree constructed from the aligned NBS domain grouped the in silico-identified TC96816 and TC98891 along with a TIR subfamily of NBS-LRR *R* genes (Fig. 1). This subfamily included well-characterized *R* genes such as the tobacco mosaic virus resistance gene *N* (A54810) and the flax rust resistance gene *L6* (U27081), as well as many of the predicted *R* genes from the *Medicago* genome. The homologous *R* gene sequences from *Medicago* spp. belong to both the TIR and non-TIR subfamilies (Fig. 1).

Table 4. (*continued from preceding page*)

TC no.[d]	EST no.	Annotation	*P* value	N/R[b]		R/R[c]	
				Fix$^+$	Fix$^-$	Nitrate	Ammonium
*TC97172	EST392162	Adaptin medium chain homolog APM2	0.0142	2.4	1.7	1.0	0.8
*TC106533	EST590785	Arbuin synthase (Hydroquinone glucosyltransferase)	0.0056	2.0	1.1	0.8	0.5
*TC112226	EST590475	β-D-glucan exohydrolase-like protein	0.006	4.1	1.3	1.4	0.5
*TC100173	EST484672	Carbonic anhydrase	0.0003	3.2	1.6	1.4	0.9
TC100309	EST483256	Enolase	0.0093	1.9	1.0	1.7	1.0
TC100309	EST483353	Enolase	0.009	1.8	1.1	1.5	0.8
*TC110318	EST590313	Sulphite reductase	0.0429	0.9	1.1	0.8	0.4
TC106510	EST315369	Glucosyltransferase-13	0.0056	3.1	1.4	0.9	0.7
TC106656	EST314917	β glucosidase-like protein	0.0004	2.8	1.9	1.1	0.6
*TC109717	EST316587	Phophatidylinosito-4-phosphate 5-kinase	0.00002	6.1	3.2	1.2	0.8
TC100321	EST393859	Phosphoglyceromutase	0.0153	2.0	1.1	0.8	0.7
*TC110571	EST485542	Type IIB calcium ATPase MCA5	0.00001	4.3	2.6	0.9	0.8
TC96792	EST333399	Urophorphyrin III methylase	0.0098	2.4	1.2	1.4	1.0
*TC95836	EST431442	DNA polymerase zeta catalytic subunit putative	0.0001	4.2	2.8	0.9	0.8
*TC104323	EST590347	Accumulation associated protein	0.0147	2.0	1.2	1.0	0.5
TC103616	EST456557	Alcohol acetyltransferase	0.012	1.6	1.4	1.2	0.6
TC107151	EST397168	Ankyrin-like protein	0.0017	3.5	1.5	0.9	0.6
TC106051	EST433469	Balbiani ring protein 1 precursor	0.0033	2.0	1.2	0.7	0.4
TC99843	EST433373	CDP-diacylglycerol-glycerol-3-phosphate 3-phosphatidyltransferase	0.0001	3.8	1.9	1.2	0.8
TC109353	EST335726	Cyclin D1	0.034	1.6	1.0	1.0	0.3
TC99981	EST458320	DEAD box RNA helicase	0.0069	3.0	1.3	1.1	0.8
TC96083	EST484912	Dynein light chain like protein	0.0019	2.9	1.4	1.4	1.2
TC101756	EST484383	Embryo-specific protein-like	0.0001	3.6	1.7	1.2	0.5
TC107181	EST393924	*Erwinia chrysanathemi* IndA protein homolog-like	0.0002	3.9	1.8	0.9	0.6
TC93945	EST430482	F1 ATPase	0.0001	3.0	2.3	1.0	0.7
TC97546	EST335118	Germin-like protein	0.0245	1.1	0.7	1.4	0.7
*TC101769	EST483169	GTP-binding protein lepA	0.0055	2.3	1.3	1.0	0.8
*TC96209	EST483595	Helicase-2	0.00005	3.8	1.4	0.8	0.4
TC102060	EST392613	Hyoscyamine 6 β-hydroxylase	0.0346	1.9	1.2	1.2	0.7
TC100554	EST457783	In2-1 protein	0.0002	3.9	2.0	1.0	0.5
*TC103185	EST483781	IRE	0.0011	2.4	1.1	1.2	0.5
TC107044	EST316006	Leucoanthocyanidin dioxygenase (LDOX)	0.0229	1.2	1.0	1.2	0.3
TC110422	EST485416	NOI protein nitrate-induced	0.0114	2.0	1.1	1.2	0.7
*TC96571	EST393387	Olfactory receptor	0.0001	4.0	1.8	1.0	0.4
TC97383	EST334452	Patatin-like protein	0.0085	0.9	0.7	1.9	0.9
*TC96633	EST483931	Pectate lyase	0.0001	3.4	1.2	2.1	0.7
*TC95550	EST483280	Probable chloroplast nucleoid DNA binding protein	0.0147	2.2	1.2	1.3	0.8
TC95664	EST433388	Protease Do-like 1	0.0366	1.8	0.9	0.8	0.8
TC94423	EST457590	Ras-related protein Rab7.	0.0017	1.8	2.0	1.2	0.5
TC94949	EST315419	Root cap protein 2 like	0.0034	2.1	1.4	0.7	0.7
TC107266	EST392523	Sedoheptulose-1 7-bisphosphatase chloroplast precursor	0.0177	1.3	0.9	1.2	0.3
*TC107078	EST331925	Sperm-specific H1/protamine-like protein type 1 precursor	0.00004	3.7	1.5	1.0	0.7
*TC105482	EST332767	cellulose synthase homolog	0.0129	2.0	1.2	1.3	0.7
*TC96476	EST393646	Putative wall associated serine/threonine kinase	0	5.2	3.0	0.8	0.7
*TC108960	EST590439	Tuftelin-interacting protein 11	0.0033	1.8	1.1	1.6	0.8

We then evaluated the 5′ end genomic region (approximately 1.5 kb upstream of the transcription start site) of three of the candidate *Medicago R* genes that were clustered with the in silico-identified TC in the phylogenetic tree: AC148918_11, AC144502_2, and AC148227_4. Analysis of the 5′ end of the putative promoter sequences revealed the presence of the AAAGAT and CTCTT motifs multiple times along the sequences, including in the inverse orientation. These consensus promoter sequences are typical of leghemoglobin gene promoters as well as several other nodulin gene promoters (Fruhling et al. 2000; Stougaard et al. 1987). Deletions or mutation analysis in the promoter regions containing the AAAGAT motif resulted in significant reduction of reporter gene expression in transgenic *Lotus* spp. and transgenic alfalfa (Szczyglowski et al. 1994; Yoshioka et al. 1999), indicating that these motifs may act as *cis*-acting elements for the expression of nodule-enhanced genes. The presence of these motifs in the homologous *R* gene sequences from *Medicago* spp. may or may not direct nodule-specific expression. Promoter activity and tissue localization of transcripts driven by these putative *Medicago R* gene promoter sequences remains to be determined.

In the array analysis, the expression of four cDNAs putatively encoding *R* genes (TC98532, TC97948, TC98670, and TC105815) was upregulated in effective nodules. These putative *R* genes also showed enhanced expression in bacterial-controlled ineffective nodules at 14 dpi (Table 2). In addition, one cDNA (TC104261), encoding putative TIR-NBS type R protein, also was enhanced in effective nodules (Table 2). A qRT-PCR analysis was performed to evaluate transcript abundance of putative *R* genes over the course of effective nodule development at 1, 3, 6, and 14 dpi. Transcript abundance of all *R* genes was significantly increased ($P < 0.05$) at 3 and 6 dpi, with expression ratios ranging from 5- to 14-fold higher than transcript abundance at 1 dpi. There were no significant differences in transcript abundance of *R* genes between 14 dpi and 1 dpi. Previously, a cDNA homologous to a resistance protein (TC90364) (Manthey et al. 2004) and two cDNAs encoding a disease resistance protein analog (Colebatch et al. 2004) were upregulated in *M. truncatula* and *Lotus* nodules at 4 and 7 weeks postinoculation, respectively. Expression of *R*-like genes in *M. truncatula* and *Lotus* nodules compared with uninoculated roots, together with the in silico identification of additional *R* gene transcripts specifically in *Medicago* nodules, indicates that *Sinorhizobium* inoculation may enhance the transcription of plant disease resistance genes in symbiotic roots and nodules. Although the functional importance of *R* gene expression in nodules is not clear, their increased transcription in effective and ineffective nodules compared with uninoculated roots and nitrate- and ammonium-fed roots suggests that they may play a role in symbiotic plant–microbe interactions.

Previously, some genes related to host defense mechanisms were shown to have no change in expression or were downregulated during nodulation of *M. truncatula*, although there were several upregulated defense response genes in nodules, including enzymes involved in secondary metabolism and defense responses (PAL, 4-coumarate:CoA ligase, chalcone reductase, cinnamyl-alcohol dehydrogenase, flavanone 3-hydroxylase, and caffeoyl-CoA-3-*O*-methyltransferase), proteins involved in cell-wall modification (glycine-rich proteins, hydroxyproline-rich proteins, and polygalacturonase inhibitor proteins) and pathogenesis-response proteins (chitinase, β-1,3-glucanase, and peroxidase) (Colebatch et al. 2004; Kouchi et al. 2004; Yahyaoui et al. 2004). Other host defense genes that showed increased expression in *M. truncatula* nodules included an *O*-methytransferase, a heat shock protein, and a putative ethylene-forming enzyme (Mitra et al. 2004). In the present array analysis, several upregulated genes in effective nodules at 14 dpi appear to encode known host stress and pathogen-responsive genes, including enzymes of the phenylpropanoid pathway, peroxidases, a superoxide dismutase, and a chitin biosynthesis protein. A cDNA encoding MtN1 protein (TC100789) also was upregulated in effective nodules, and enhanced transcript abundance also was detected in ineffective nodules (Table 3). In a previous study, MtN1 and MtN13, encoding proteins structurally related to a cysteine-rich pathogen-inducible and the PR10 family of plant defense proteins, respectively, were identified in *S. meliloti* and *M. truncatula* interactions (Gamas et al. 1998). Because these classes of genes are induced as part of plant defense to stress and pathogen attack, their enhanced expression in effective nodules may signify an induction by legume plants of common proteins for bacterial symbiosis as well as host defense response. It also is possible that these proteins may have a function not related to a defense response in developing and N-fixing nodules.

Other nodule-enhanced genes from our in silico and cDNA array analyses include cysteine proteases and proteinase inhibitors. The identification and cloning of a gene encoding a secreted cysteine protease (Rcr3) that is required for *Cladosporium fulvum* resistance, and a secreted aspartic protease (CDR1)

Table 5. Validation of cDNA array results with quantitative reverse-transcription polymerase chain reaction (qRT-PCR)[a]

				N/R[b]			
				Macroarray		qRT-PCR	
TC no.[c]	EST no.	Annotation	*P* value	Fix^+	Fix^-	Fix^+	Fix^-
*TC101825	MTNAK80TKM	ENOD12	0.00004	4.4	2.5	17.9	5.5
*TC107339	EST391681	ENOD18	0.0095	2.2	1.2	36.2	10.0
*TC100731	EST485371	ENOD20	0.0140	2.3	1.8	15.6	5.9
TC100789	EST391799	MtN1	0.0010	3.7	1.9	10.5	4.4
*TC100596	EST484646	MtN22	0.0021	2.3	1.5	32.9	18.5
*TC95958	EST484918	MtN26	0.0038	2.7	1.5	15.2	8.9
*TC108339	EST485161	MtN28	0.0453	1.4	1.0	14.7	16.5
*TC107188	EST484058	MtN29	0.0011	2.7	1.7	11.2	8.9
TC101065	EST429437	Nodule-specific glycine-rich protein 2A	0.0026	2.8	2.1	0.9	0.8
*TC106696	EST393913	Nodulin 25	0.0002	2.9	1.3	30.1	9.0
*TC108713	EST483740	No annotation	0.0057	3.9	1.9	29.4	13.3
TC95706	EST393917	No annotation	0.0004	2.0	1.7	39.7	20.4
*TC109907	EST331932	No annotation	0.0385	3.5	1.5	0.4	0.3

[a] Tentative consensus sequence (TC) and expressed sequence tag (EST) numbers correspond to The Institute for Genomic Research *Medicago truncatula* Gene Index version 8.

[b] N/R denotes mean nodule/uninoculated root expression ratio for effective nodules (Fix^+) and ineffective nodules (Fix^-).

[c] Asterisk (*) indicates identified as *Sinorhizobium* inoculated tissue-specific by in silico analysis.

that regulates an inducible resistance response (Kruger et al. 2002; Xia et al. 2004), suggest that plant proteases are involved in host defense. Therefore, it may be argued that proteases and proteinase inhibitors could potentially protect the nodule tissue from pathogen and pest attack.

With regard to cysteine-cluster containing proteins, Fedorova and associates (2002) and Mergaert and associates (2003) identified in silico at least 150 TC encoding small proteins (60 to 100 amino acids) with conserved cysteine-rich regions and a signal peptide at the N-terminal region of the protein (CCPs). Despite deeper sequencing, many of these CCPs (109 TC composed of 660 EST) are clustered from EST derived exclusively from inoculated root and nodule cDNA libraries. Approximately 93% of these TCS are clustered from EST prepared exclusively from N-fixing and senescent nodules, whereas approximately 2% are assembled from EST prepared from inoculated root cDNA libraries. Many of the in silico-identified CCPs are composed of five or more EST per TC. The array analysis showed that approximately 71% of the spotted CCPs were strongly induced in effective and bacterial-conditioned ineffective nodules. Enhanced expression in bacterial-controlled ineffective nodules suggests that symbiosis-specific CCPs play a role in a process other than nitrogen metabolism in nodules. Motif analysis of CCPs has revealed strong similarities to plant defensins, some of which confer resistance against plant pathogens (Graham et al. 2004). Mergaert and associates (2004) also suggested that symbiosis-specific CCPs might function in cellular defense or cell-to-cell signaling during nodulation.

With regard to signal transduction in N-fixing nodules, Colebatch and associates (2004) identified approximately 43

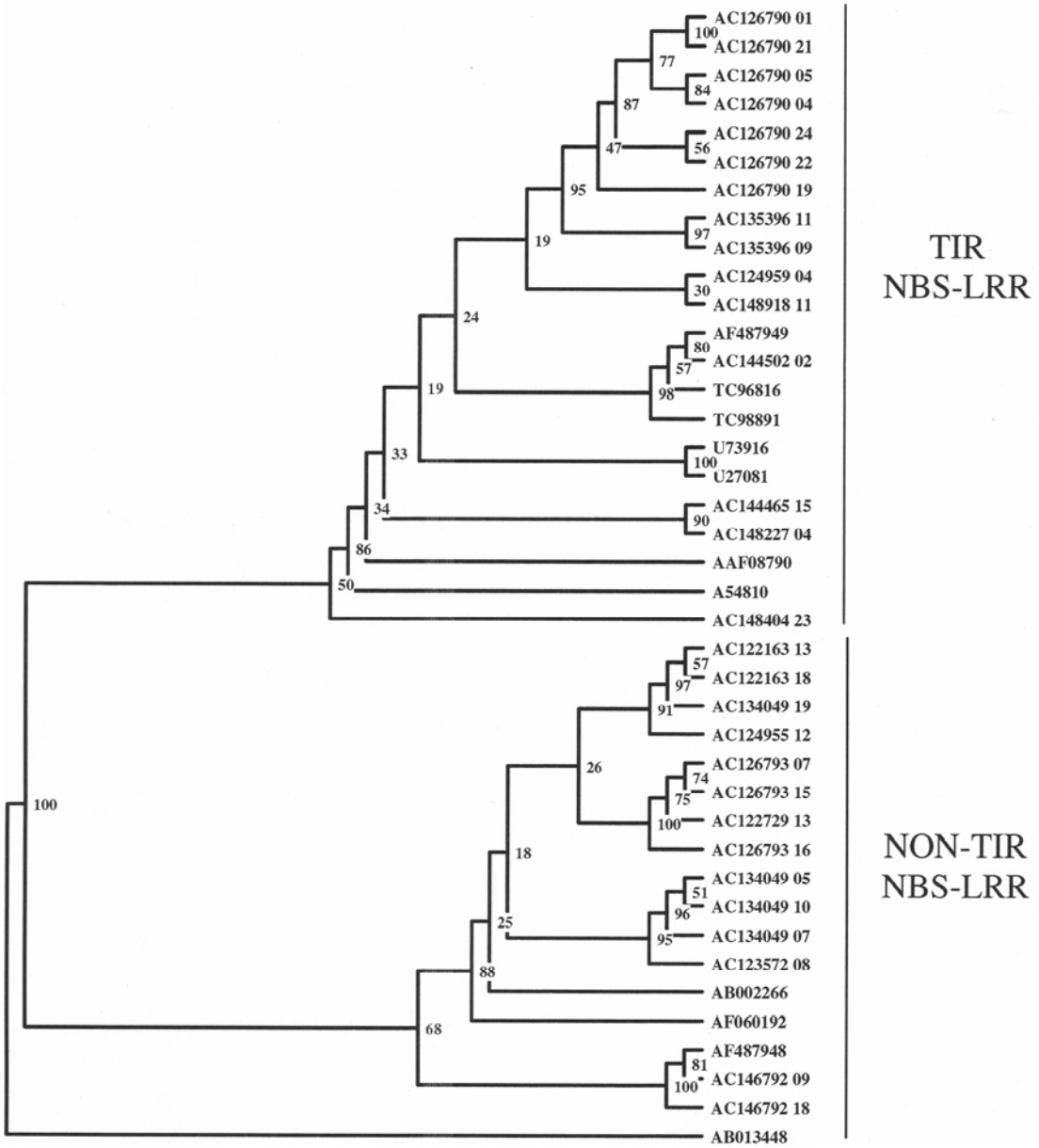

Fig. 1. Parsimony tree of plant disease resistance (*R*) genes. In silico-identified TC96816 and TC98891 and 29 *R* gene sequences from the *Medicago* genome were aligned with nucleotide binding site (NBS) sequences of known *R* genes from the toll and interleukin-1 receptor (TIR) and non-TIR classes. Accessions numbers for known *R* genes are: *Medicago sativa* NBS–leucine-rich repeat (LRR)-Toll resistance gene analog (AF487949), *Tobacco mosaic virus* resistance gene *N* of *Nicotiana glutinosa* (A54810), downy mildew resistance protein RPP5 of *Arabidopsis thaliana* (AAF08790), *Linum usitatissimum* rust resistance gene *L6* (U27081), *L. usitatissimum* rust resistance protein *M* gene (U73916), *Oryza sativa* bacterial blight-resistance gene *Xa*1 (AB002266), *Glycine max* putative resistance protein *KNBS*4 gene (AF060192), the *Pib* gene for rice blast resistance (AB013448), and *M. ruthenica* isolate R625NBSD NBS-LRR-non-Toll resistance gene analog protein (AF487948). The numbers on tree branches indicate bootstrap values based on 100 bootstrap resamplings.

genes in *Lotus* spp. In the present study, a total of 31 TC assembled from 131 EST exclusively from *Sinorhizobium*-inoculated tissues showed homology to genes involved in signal transduction, although only 6 TC were clustered from 5 or more EST. One unique group of signal transduction transcripts identified by Fedorova and associates (2002) contains the CaM-like genes. Eight CaM-like TC originally identified by Fedorova and associates (2002) (TC99375, TC107257, TC107926, TC101807, TC96504, TC102961, TC95911, and TC99193) were derived exclusively from inoculated root and nodule cDNA libraries. In the array analysis, CaM-like proteins showed differential expression patterns: those that were upregulated in effective and ineffective nodules (CaM-like 1, CaM-like 3, and CaM-like 5), and those cDNAs upregulated in effective nodules and also enhanced in ineffective nodules (CaM-like 2 and CaM-like 6b) (Table 2). The nodule-enhanced CaM-like proteins appear to localize in the symbiosome space of *M. truncatula* nodules (J. Liu, J. Sherrier, B. Buccairelli, and C. P. Vance, *unpublished*). Nevertheless, their functional importance in nodules remains to be established.

Another group of in silico-identified TC that may play a role in signal transduction putatively encode several protein kinases (TC104400, TC104745, TC106116, TC98207, TC104545, TC97492, TC99256, TC111529, and TC108845), eight TC encoding transcription factors as well as a remorin-like protein (TC96630). In the cDNA array analysis, cDNAs representing an S glycoprotein (TC103882), a protein kinase homolog NPK1 (TC106116), and transcription factor (TC99871 and TC95981) proteins showed upregulated expression in Nod^+Fix^+ nodules (Table 2).

Is there a role for neutral invertase in *Medicago* nodules?

Sucrose cleavage to hexose is the first step in carbon use by nodules for symbiotic nitrogen fixation. Plants degrade sucrose through either sucrose synthase or invertase (Strum 1999; Strum and Tang 1999). In the array analysis, a cDNA for neutral invertase (TC106499) showed upregulated expression in effective nodules at 14 dpi compared with uninoculated roots (Table 4). A qRT-PCR analysis was performed to evaluate transcript abundance of invertase over the course of effective nodule development at 1, 3, 6, and 14 dpi. There were significant increases in transcript abundance of invertase at 3, 6, and 14 dpi ($P < 0.05$). Expression ratios of invertase at 3, 6, and 14 dpi were 15-, 11- and 4-fold higher, respectively, than transcript abundance at 1 dpi. Previous evidence suggests a role for neutral invertase in nodules. Manthey and associates (2004) showed upregulated expression of neutral invertase in root nodules of *M. truncatula.* Enhanced expression and enzyme activities of invertase and sucrose synthase genes in root nodules of *M. truncatula,* pea, and lentil were reported previously, indicating that both genes are active in N-fixing nodules (Chopra et al. 2003; Craig et al. 1999; Gordon et al. 1999; Yahyaoui et al. 2004). On the other hand, increased expression of sucrose synthase was observed in root nodules of *M. truncatula* and *Lotus* spp. (Colebatch et al. 2004; Hohnjec et al. 1999; Kouchi et al. 2004). The presence of isozyme forms of sucrose synthases and invertases with contrasting carbohydrate responsiveness may explain the differences in their expression profiles in *M. truncatula* nodules (Kouch 1996). Differences in expression profiles also may be due to differences in the timing of root tissue harvest relative to the stage of nodule development. In contrast to sucrose synthase, little is known about neutral invertase activity in *M. truncatula* nodules. Further work is warranted to establish the unequivocal roles of sucrose synthase and neutral invertase during nodule development in *M. truncatula*.

Organic acid synthesis and nitrogen metabolism genes are coexpressed in nitrate-treated roots and N-fixing nodules of *Medicago* spp.

Plants obtain nitrogen via a number of ways: through symbiotic nitrogen fixation and nitrate reduction in roots and shoots, among others (Vance 1997). Irrespective of the primary source, N is first reduced to NH_4^+ before it is assimilated into the amino acids glutamine and glutamate, which serve to translocate organic N from source tissues to sink tissues (Vance 1997). Ammonium is synthesized from nitrate by the actions of the nitrate assimilation genes, nitrate reductase, and nitrite reductase (Crawford 1995) and, hence, the upregulation of these genes by nitrate is expected. The major genes involved in primary N-assimilation are glutamine synthetase (GS), glutamate synthase (GOGAT), aspartate aminotransferase (AAT), and asparagine synthase (AS) (Vance 1997; Vance et al. 1994). The transcription response of *M. truncatula* to nitrate and ammonium addition has not been investigated previously. However, DNA arrays used to identify *Arabidopsis* and tomato genes that respond to nitrate following a period of N deficiency identified over 1,000 induced genes, including several nitrate transporter gene families and nitrate assimilation genes (Scheible et al. 2004; Wang et al. 2001, 2003). N-assimilation genes such as GS, GOGAT and AS were induced by nitrate in *Arabidopsis* and tomato (Scheible et al. 2004; Wang et al. 2001, 2003). Expression of genes encoding phosphoenolpyruvatecarboxylase (PEPC), cytosolic pyruvate kinase, citrate synthase (CS), and NADP-isocitrate dehydrogenase were induced in tobacco, *Arabidopsis,* and tomato plants supplied with nitrate when compared with control roots (Scheible et al. 1997; Wang et al. 2001, 2003). Nitrate also induced PEPC kinase, carbonic anhydrase (CA), peroxidase, aconitases, enolase, cytoplasmic malate dehydrogenase (MDH), aquaporins, root phosphate, and potassium transporters in *Arabidopsis* and tomato plants (Scheible et al. 2004; Wang et al. 2001, 2003). The macroarray results of *M. truncatula* were similar to the nitrate responses of *Arabidopsis*, tobacco, or tomato plants in that PEPC kinase (TC108608), MDH (TC107189), NADH-GOGAT (TC94780), AS (TC100391 and TC100393), nitrite reductase (TC100672), and GS (TC106913) were upregulated in *M. truncatula* roots following the supply of 5 mM nitrate to N-limited plants (Table 4). In addition, PEPC (TC94196), succinyl-CoA synthase (TC101044), CS (TC95758), MDH (TC94390, TC100429, and TC100430), and enolase (TC100309) showed enhanced expression in nitrate-fed roots of *M. truncatula* (Table 4). However, nitrate induced several invertases in *Arabidopsis,* whereas none of the six-member sucrose synthase family was induced (Scheible et al. 2004). By contrast, we found upregulated expression of two cDNAs of a sucrose synthase gene (TC100410) and enhanced expression of a fructokinase gene (TC94345) in nitrate-treated *M. truncatula* roots compared with control roots (Table 4).

In N-fixing nodules, the carbon skeletons required for initial assimilation of ammonium (Vance 1997; Vance et al. 1994) and the predominant sources of energy for bacteroid respiration (Driscoll and Finan 1993) are derived from organic acids. In the presence of CA and PEPC, phosphoenolpyruvate (PEP) is transformed to oxaloacetate, which then can be reduced to malate by MDH (Miller et al. 1997; Vance et al. 1994). In keeping with these observations, transcripts for CA (TC94246 and TC100173) and MDH (TC94390 and TC107189) showed upregulated expression in effective nodules of *M. truncatula* at 14 dpi (Table 4). Also, transcripts for PEPC (TC94196) and two cDNAs of CS (TC95758 and TC107007) showed enhanced expression in effective nodules of *M. truncatula* at 14 dpi (Table 4). These results are consistent with previous observations that the enzymes that utilize citric acid intermediates showed the

highest enzyme activity levels in the plant fraction of alfalfa nodules (Irigoyen et al. 1990). The expression of MDH, CA, and PEPC also were increased in effective nodules of *Lotus* spp. (Colebatch et al. 2004). In general, transcript abundance of genes involved in primary N assimilation were increased during effective nodule development of *M. sativa*, *M. truncatula,* and *Lotus* spp. and generally were reduced in bacterial-controlled ineffective nodules of *M. sativa* (Colebatch et al. 2004; Gantt et al. 1992; Kouchi et al. 2004; Vance et al. 1994; Yahyaoui et al. 2004). Consistent with these reports, transcripts of GS, AS, amino transferase, and nitrite reductase were expressed strongly in effective nodules of *M. truncatula* at 14 dpi (Table 4). Our observations and those of others, that show that genes for organic acid synthesis and N metabolism are coexpressed in nodules, further strengthens the argument that N and C metabolic pathways are highly integrated during effective bacterial symbiosis and play a vital role in providing C skeletons during N assimilation.

Concluding remarks.

We updated the list of *Medicago* TC clustered exclusively from *Sinorhizobium*-inoculated root and nodule EST previously reported by Fedorova and associates (2002) and employed a cDNA array analysis to verify their induced transcription in effective nodules, S*inorhizobium*-controlled ineffective nodules, and nitrate- and ammonium-fed roots of N-starved plants. The updated list of in silico-identified TC is expected to be a valuable resource for the *Medicago* community. The present study shows that some of the in silico-identified TC also are induced in *Sinorhizobium*-controlled ineffective nodules. The study reported here and others with *M. truncatula* and *Lotus* spp. suggest that rhizobia–plant symbiosis may share features in common with plant–pathogen interactions and, perhaps, show a parallel between plant responses to symbionts and pathogens. Plants interact with soil microorganisms throughout their life cycle. To control the number of effective nodules formed and to avoid nonsymbiotic infections, the host plant must assess the process of bacterial interaction and nodulation at all times and should trigger host resistance strategies should a microbial interaction fail to move toward symbiosis. The challenge for researchers is to identify the crucial differences in plant responses to symbiotic and pathogenic microorganisms that result in different outcomes. Because a large number of selected probes can be evaluated in parallel, custom-made arrays with EST from the model *M. truncatula* such as reported here give further insights into N and C metabolism in nodules. By contrasting expression in bacterial-conditioned nodule forms, the cDNA array data provides conclusive support for earlier suggestions by many workers that C and N metabolism genes are coexpressed in effective nodules. Furthermore, published results from array analysis of transcripts from determinate and indeterminate nodules using the two model legumes, *Lotus japonicus* and *M. truncatula,* respectively, reveal remarkable agreement for expression of most nodule-enhanced genes and provide impetus for future gene-silencing studies. Detailed study on changes in metabolite concentrations should compliment results from cDNA filter array data and help rectify contrasting results. We conclude that results obtained from applying genomics tools to identify genes associated with symbiotic nitrogen fixation and mineral N nutrition in *M. truncatula* should be transferable to other herbaceous legume species.

MATERIALS AND METHODS

In silico analysis.

Release 8.0 of the *M. truncatula* EST collection at TIGR contains 18,612 TC clustered from 208,685 EST. An in silico analysis was applied to identify those TC composed of EST exclusively from effective *S. meliloti*-inoculated roots and nodules of *M. truncatula* genotypes A17 and R108, as described previously (Fedorova et al. 2002).

Plant culture and growth conditions.

M. truncatula genotype A17 seed were scarified and sown in pots containing a 1:1 (vol/vol) mixture of vermiculite and industrial quartz (Unimin Corporation, New Cannan, CT, U.S.A.) which had been mixed with an N-free nutrient solution (Vincent 1970). Four days after seedling emergence, when the primary leaf was fully open, seedlings were inoculated with a suspension of *S. meliloti* strain 102F51 or *S. meliloti* mutant strain T202 in distilled water. The inoculants were prepared from early stationary phase cultures grown in yeast mannitol broth (Vincent 1970). Reference treatments were inoculated with distilled water. The experiment was conducted in a growth chamber (temperature cycle of 21 and 19ºC, light and dark, with a 14-h light cycle) with three replicates in each treatment. Plants were watered with N-free nutrient solution throughout the experiment. Root and nodule samples were collected by hand, placed on dry ice, ground in liquid nitrogen, and stored at –80ºC. Transcription patterns for the inoculation experiment were evaluated between roots of uninoculated control and effective or ineffective nodules of *Sinorhizobium*-inoculated plants that grew in parallel for 14 dpi.

For N fertilizer treatments, *M. truncatula* cv. A17 seed were scarified and sown in pots containing a 1:1 (vol/vol) mixture of vermiculite and industrial quartz which had been mixed with an N-free nutrient solution (Vincent 1970). Plants were grown in N-free nutrient solution for 20 days after seedling emergence before they received 5 mM nitrate as KNO_3, or 5 mM ammonium as NH_4SO_4 for 24 h. Reference treatments received 5 mM KCl for 24 h. Root samples were collected by hand, placed on dry ice, ground in liquid nitrogen, and stored at –80ºC. Gene expression patterns between roots of nitrate- or ammonium-fed plants were evaluated with roots of KCl-fed (control) plants 24 h after treatment.

Preparation of macroarrays.

The cDNA inserts were amplified by PCR with T3 and T7 primers and the quality of each PCR product was evaluated by agarose gel electrophoresis. PCR products were arrayed on Gene Screen Plus membranes using a Q-bot (Genetix, Boston, U.S.A.) fitted with a 96-pin gravity gridding head, essentially as described previously (Uhde-Stone et al. 2003). Each EST was spotted in duplicate on each filter array. Arrayed filters were air dried and stored at room temperature. DNA was denatured for 10 min by placing filters cDNA side up on Whatman 3 MM paper soaked with denaturing solution (1.5 M NaCl and 0.5 M NaOH), followed by 5 min on Whatman 3 MM paper soaked with neutralization solution (1.5 M NaCl and 1 M Tris, pH 8.0). Filters were air dried and fixed by UV cross-linking (120 joules cm^{-2}).

RNA extraction, hybridization, data acquisition, and analysis.

Total RNA was extracted from nodule and root tissues using the RNeasy Plant RNA mini kit (Qiagen, Valencia, CA, U.S.A.) following the manufacturer's instructions. For hybridization, α-^{32}P-dATP-labeled first-strand cDNAs were synthesized by reverse transcription of 30 µg of total RNA with the Superscript RT II kit (Invitrogen, Carlsbad, CA, U.S.A.), oligo$(dT)_{12–18}$ (Sigma-Aldrich, St. Louis), and dNTPs mix as described previously (Fedorova et al. 2002). Unincorporated nucleotides were removed by passing the mixture through Micro Bio-Spin Chromatography Columns (Bio-Rad, Hercules, CA,

U.S.A.) and ^{32}P incorporation was quantified via liquid scintillation counting. The final concentration of each labeled first-strand cDNA was adjusted to 1×10^6 cpm/ml of hybridization solution. Filters were hybridized and washed as described previously (Fedorova et al. 2002; Uhde-Stone et al. 2003). There were three replicate filters derived from three completely randomized replicate treatments as described above. Hybridized filters were wrapped in plastic and exposed to phosphor screens for 5 days. Phosphor screens were scanned using the storm 840 PhosphoImager (Molecular Dynamics). The fluorescence intensity of each spot was quantified automatically using the Array-Pro analysis software (version 1.0; Media Cybernetics, Carlsbad, CA, U.S.A.). The local background was subtracted from the intensity values for each spot. Mean signal intensity for each spotted EST was calculated from the duplicate spots on each filter. Gene expression ratios of nodules to uninoculated control roots as well as gene expression ratios for the nitrate- and ammonium-fed roots to control roots of KCl-fed plants were calculated. Array data was normalized and analyzed using GeneSpring (version 7.2; Silicon Genetics, Redwood City, CA, U.S.A.) as provided by the Supercomputing Institute of the University of Minnesota. ANOVA was performed with *P* value cutoff at 0.05.

qRT-PCR analysis.

Total RNA was treated with RQ DNAse I (Promega Corp., Madison, WI, U.S.A.) at 37ºC for 1 h to remove any contaminating DNA, and then total RNA was isolated using a spin column provided as part of the RNeasy Plant RNA minikit (Qiagen). First-strand cDNA was prepared from 2 µg of total RNA with the Superscript RT II kit (Invitrogen) and random hexamers (Sigma-Aldrich) at 200 ng/reaction, according to the manufacturer's instructions.

Gene-specific primers for the RT-PCR analysis were designed using the PrimerExpress software (Applied Bisosystems, Foster City, CA, U.S.A.). A PCR master mixture using the SYBR Green PCR and RT-PCR Reagents (Applied Biosystems) was mixed with 1.5 µl of first-strand cDNA as template, 40 pmol each primer for a final volume of 25 µl per reaction. The ABI PRISM 7000 Sequence Detection System (Applied Biosystems) was used for the PCR and detection of the fluorescent signal. Cycle conditions were 1 cycle of 50ºC for 2 min and 1 cycle of 95ºC for 10 min, followed by 40 cycles of 95ºC for 15 s and 60ºC for 1 min. The analysis was performed in triplicate. The specificity of the RT-PCR reaction products was confirmed by running a heat-dissociation curve after the end of the PCR reaction, as well as by agarose gel electrophoresis. Primers specific for the *M. truncatula* 18S rRNA were used as an endogenous control to account for variability in the initial concentration and quality of the total RNA. For data analysis, gene expression was normalized to the 18S rRNA expression levels in each sample. The calibrator sample in real-time RT-PCR was the cDNA from the root samples of uninoculated control plants that received a nitrogen free nutrient solution. The threshold cycle ($\Delta\Delta$CT) method of comparing expression data was applied and the relative quantitative value was expressed as $2^{-\Delta\Delta CT}$.

ACKNOWLEDGMENTS

This article is a joint contribution from the University of Minnesota and the Plant Science Research Unit, United States Department of Agriculture (USDA)–Agricultural Research Service. Mention of a trademark, proprietary product, or vendor does not constitute a guarantee or warranty of the product by the USDA, and it does not imply its approval to the exclusion of other products and vendors that might also be suitable. We thank W. Xu of the Supercomputing Institute, University of Minnesota, for assistance in advanced GeneSpring Analysis of the array data.

LITERATURE CITED

Appleby, C. A. 1984. Leghemoglobins and *Rhizobium* respiration. Annu. Rev. Plant Physiol. 35:443-478.

Chopra, J., Kaur, N., and Gupta, A. K. 2003. Changes in sugar content and activities of sucrose metabolizing enzymes in roots and nodule of lentil. Biol. Plant. 46:89-93.

Colebatch, G., Desbrosses, G., Ott, T., Krusell, L., Montanari, O., Kloska, S., Kopka, J., and Udvardi, M. 2004. Global changes in transcription orchestrate metabolic differentiation during symbiotic nitrogen fixation in *Lotus japonicus*. Plant J. 39:487-512.

Cook, D. R. 1999. *Medicago truncatula*: a model in the making. Curr. Opin. Plant Biol. 2:301-304.

Craig, P., Barratt, P., Tatge, H., Dejardin, A., Handley, L., Gaardner, C. D., Wang, T., Hedley, C., Martin, C., and Smith, A. M. 1999. Mutations in the *rug4* locus alter the carbon and nitrogen metabolism of pea plants through an effect on sucrose synthase. Plant J. 17:353-362.

Crawford, N. M. 1995. Nitrate: nutrient and signal for plant growth. Plant Cell 7:859-868.

Driscoll, B. T., and Finan, T. M. 1993. NAD+-dependent malic enzyme of *Rhizobium meliloti* is required for symbiotic nitrogen fixation with *Medicago sativa*. Mol. Microbiol. 7:865-875.

Fedorova, M., van de Mortel, J., Matsumoto, P. A., Cho, J., Town, C. D., VandenBosch, K. A., Gantt, J. S., and Vance, C. P. 2002. Genome-wide identification of nodule-specific transcripts in the model legume *Medicago truncatula*. Plant Physiol. 130:519-537.

Fruhling, M., Hohnjec, N., Schroder, G., Kuster, H., Puhleer, A., and Perlick, A. M. 2000. Genomic organization and expression properties of the *VfENOD5* gene from broad bean (*Vicia faba* L.). Plant Sci. 155:169-178.

Gamas, P., de Billy, F., and Truchet, G. 1998. Symbiosis-specific expression of two *Medicago truncatula* nodulin genes, MtN1 and MtN13, encoding products homologous to plant defense proteins. Mol. Plant-Microbe Interact. 11:393-403.

Gantt, J. S., Larson, R. L., Farnham, M. W., Pathirana, S. M., Miller, S. S., and Vance, C. P. 1992. Aspartate aminotransferase in effective and ineffective alfalfa nodules. Plant Physiol. 98:868-878.

Gordon, A. J., Minchin, F. R., James, C. L., and Komina, O. 1999. Sucrose synthase in legume nodules is essential in nitrogen fixation. Plant Physiol. 120:867-877.

Graham, M. A., Silverstein, K. A. T., Cannon, S. B., and VandenBosch, K. A. 2004. Computational identification and characterization of novel genes from legumes. Plant Physiol. 135:1179-1197.

Hohnjec, N., Becker, A., Puhler, A., Perlick, A. M., and Kuster, H. 1999. Genomic organization and expression properties of the *MtSuc*1 gene, which encodes a nodule-enhanced sucrose synthase in the model legume *Medicago truncatula*. Mol. Gen. Genet. 261:514-522.

Irigoyen, J. J., Sanchez-Diaz, M., and Emerich, D. W. 1990. Carbon metabolism enzymes of *Rhizobium meliloti* cultures and bacteroids and their distribution within alfalfa nodules. Appl. Environ. Microbiol. 56:2587-2589.

Journet, E. P., van Tuinen, D., Gouzy, J., Crespeau, H., Carreau, V., Farmer, M. J., Niebel, A., Schiex, T., Jaillon, O., Chatagnier, O., Godiard, L., Micheli, F., Kahan, D., Gianinazzi-Pearson, V., and Gamas, P. 2002. Exploring root symbiotic programs in the model legume *Medicago truncatula* using EST analysis. Nucleic Acids Res. 30:5579-5592.

Kouch, K. E. 1996. Carbohydrate-modulated gene expression in plants. Annu. Rev. Plant Physiol. Plant Mol. Biol. 47:509-540.

Kouchi, H., Shimomur, K., Hata, S., Hirota, A., Wu, G. J., Kumagai, H., Tajima, S., Suganuma, N., Suzuki, A., Aoki, T., Hayashi, M., Yokoyama, T., Ohyama, T., Asamizu, E., Kuwta, C., Shibata, D., and Tabata, S. 2004. Large-scale analysis of gene expression profiles during early stages of root nodule formation in a model legume, *Lotus japonicus*. DNA Res. 11:263-274.

Kruger, J., Thomas, C. M., Golstein, C., Dixon, M. S., Smoker, M., Tang, S., Mulder, L., and Jones, J. D. G. 2002. A tomato cysteine protease required for *Cf-2*-dependent disease resistance and suppression of autonecrosis. Science 296:744-747.

Manthey, K., Krajinski, F., Hohnjec, N., Firnhaber, C., Puhler, A., Perlick A. M., and Kuster, H. 2004. Transcriptome profiling in root nodules and arbuscular mycorrhizal identifies a collection of novel genes induced during *Medicago truncatula* root endosymbioses. Mol. Plant-Microbe Interact. 17:1063-1077.

Mergaert, P., Nikovics, K., Kelemen, Z., Maunoury, N., Vauber, D., Kondorosi, A, and Kondorosi, E. 2003. A novel family in *Medicago truncatula* consisting of more than 300 nodule-specific genes coding for small, secreted polypeptides with conserved cysteine motifs. Plant Physiol. 132:161-173.

Meyers, B. C., Dickerman, A. W., Michelmore, R. W., Sivaramakrishnan, S., Sobral, B. W., and Young, N. D. 1999. Plant disease resistance genes

encode members of an ancient and diverse protein family within the nucleotide-binding superfamily. Plant J. 20:317-332.
Miller, S. S., Driscoll, B. T., Gregerson, R. G., Gantt, J. S., and Vance, C. P. 1997. Alfalfa malate dehydrogenase (MDH): molecular cloning and characterization of five different forms reveals a unique nodule-enhance MDH. Plant J. 15:173-184.
Mithofer, A. 2002. Suppression of plant defense in rhizobia-legume symbiosis. Trends Plant Sci. 7:440-444.
Mitra, R. M., Shaw, S. L., and Long, S. R. 2004. Six nonnodulating plant mutants defective for Nod factor-induced transcriptional changes associated with the legume-rhizobia symbiosis. Proc. Natl. Acad. Sci. U.S.A. 101:10217-10222.
Ott, T., van Dongen, J. T., Gunther, C., Krusell, L., Desbrosses, G., Vigeolas, H., Bock, V., Czechowski, T., Geigenberger, P., and Udvardi, M. 2005. Symbiotic leghemoglobins are crucial for nitrogen fixation in legume root nodules but not for general plant growth and development. Curr. Biol. 15:531-535.
Scheible, W. R., Gonzalez-Fontes, A., Lauerer, M., Muller-Ruber, B., Caboche, M., and Stitt, M. 1997. Nitrate acts as a signal to induce organic acid metabolism and repress starch metabolism in tobacco. Plant Cell 9:783-798.
Scheible, W. R., Morcuende, R., Czechowski, T., Fritz, C., Osuna, D., Palacios-Rojas, N., Schindelasch, D., Thimm, O., Udvardi, M. K., and Stitt, M. 2004. Genome-wide reprogramming of primary and secondary metabolism, protein synthesis, cellular growth process, and the regulation of infrastructure of *Arabidopsis* response to nitrogen. Plant Physiol. 136:2483-2499.
Stougaard, J., Sandal, N. N., Groen, A., Kuhle, A., and Marcker, K. A. 1987. 5′ analysis of the soybean leghemoglobin *lbc3* gene: regulatory elements required for promoter activity and organ specificity. EMBO (Eur. Mol. Biol. Organ.) J. 6:3565-3569.
Strum, A. 1999. Invertase. Primary structures, functions, and roles in plant development and sucrose partitioning. Plant Physiol. 121:1-7.
Strum, A., and Tang, G. Q. 1999. The sucrose-cleaving enzymes of plants are crucial for development, growth and carbon partitioning. Trends Plant Sci. 4:401-407.
Szczyglowski, K., Szabados, L., Fujimoto, S. Y., Silver, D., and de Bruijn, F. J. 1994. Site-specific mutagenesis of the nodule-infected cell expression (NICE) element and the AT-rich element ATRE-BS2 of the *Sesbania rostrata* leghemoglobin *glb*3 promoter. Plant Cell 6:317-332.
Thoquet, P., Gherardi, M., Journet, E. P., Kereszt, A., Ane, J. M., Prosperi, J. M., and Huguet, T. 2002. The molecular genetic linkage map of the model legume *Medicago truncatula*: an essential tool for comparative legume genomics and the isolation of agronomically important genes. BMC Plant Biol. 2:1
Uhde-Stone, C., Zinn, K. E., Ramirez, Y. M., Li, A. G., Vance, C. P., and Allan, D. L. 2003. Nylon filter arrays reveal differential gene expression in proteoid roots of white lupin in response to phosphorus deficiency. Plant Physiol. 131:1064-1079.
Vance, C. P. 1997. The molecular biology of N-metabolism. Pages 449-477 in: Plant Metabolism. D. T. Dennis, D. H. Turpin, D. D. Lefebvre, and D. B. Layzell, eds., Longman, London.
Vance, C. P., Gregerson, R. G., Robinson, D. L., Miller, S. S., and Gantt, J. S. 1994. Primary assimilation of nitrogen in alfalfa nodules: molecular features of the enzymes involved. Plant Sci. 101:51-64.
Vincent, J. M. 1970. A manual for the practical study of root-nodule bacteria. IBP Handbook No. 15. Blackwell Scientific Publications, Oxford.
Virts, E. L., Stanfield, S. W., Helinski, D. R., and Ditta, G. S. 1988. Common regulatory elements control symbiotic and microaerobic induction of *nif*A in *Rhizobium meliloti*. Proc. Natl. Acad. Sci. U.S.A. 85:3062-3065.
Wang, R. C., Okamoto, M., Xing, X., and Crawford, N. M. 2003. Microarray analysis of the nitrate response in *Arabidopsis* roots and shoots reveals over 1000 rapidly responding genes and new linkages to glucose, trehalose-6-phosphate, iron, and sulfate metabolism. Plant Physiol. 132:556-567.
Wang, Y. H., Garvin, D. F., and Kochian, L. V. 2001. Nitrate-induced genes in tomato roots. Array analysis reveals genes that may play a role in nitrogen nutrition. Plant Physiol. 127:345-359.
Xia, Y., Suzuki, H., Borevitz, J., Blount, J., Guo, Z., Patel, K., Dixon, R. A., and Lamb, C. 2004. An extracellular aspartic protease functions in *Arabidopsis* disease resistance signaling. EMBO (Eur. Mol. Biol. Organ.) J. 23:980-988.
Yahyaoui, F. E., Kuster, H., Amor, B. B., Hohnjec, N., Puhler, A., Becker, A., Gouzy, J., Vernie, T., Gough, C., Niebel, A., Godiard, L., and Gamas, P. 2004. Expression profiling in *Medicago truncatula* identifies more than 750 genes differentially expressed during nodulation, including many potential regulators of the symbiotic program. Plant Physiol. 136:3159-3176.
Yoshioka, H., Gregerson, R. G., Samac, D. A., Hoeven, K. C. M., Trepp, G., Gantt, J. S., and Vance, C. P. 1999. Aspartate aminotransferase in alfalfa nodules: localization of mRNA during effective and ineffective nodule development and promoter analysis. Mol. Plant-Microbe Interact. 12:263-274.
Zhou, H., Cannon, S. B., Young, N. D., and Cook, D. R. 2002. Phylogeny and genomic organization of the TIR and Non-TIR NBS-LRR resistance gene family in *Medicago truncatula*. Mol. Plant-Microbe Interact. 15:529-539.

AUTHOR-RECOMMENDED INTERNET RESOURCES

The Institute for Genomic Research (TIGR) *Medicago* Gene Index: www.tigr.org/tdb/mtgi
TIGR *Medicago truncatula* database: www.medicago.org